

## P8.26

## PRECIPITATION CHARACTERISTICS OF SUPERCELL HOOK ECHOES

Matthew R. Kumjian\* and Alexander V. Ryzhkov

National Severe Storms Laboratory, Cooperative Institute for Mesoscale Meteorological Studies, and Atmospheric Radar Research Center, University of Oklahoma, Norman, OK

## 1. INTRODUCTION

Recent studies have suggested that thermodynamic properties of supercell rear-flank downdrafts (RFDs) can affect whether or not tornadogenesis occurs. Observational studies by Markowski et al. (2002) and Grzych et al. (2007) demonstrate that supercells which produced significant tornadoes had rear-flank downdrafts with smaller equivalent potential temperature deficits and virtual potential temperature deficits than the RFDs of weakly tornadic or nontornadic supercells. Idealized numerical simulations by Markowski et al. (2003) support these findings, suggesting that excessively cold RFDs are associated with relatively weak surface convergence that cannot stretch vertical vorticity to tornadic magnitudes. Another possibility is that excessively cold (large negative buoyancy) RFDs “gust out” to the extent that the incipient vortex (which develops along the RFD gust front) is not in an optimal position to be strengthened via convergence beneath the intense low-level updraft.

The thermodynamic characteristics of rear-flank downdrafts are determined in part by microphysical processes such as evaporation of raindrops and melting of hailstones. Whereas in situ measurements of changes in the hook echo particle size distributions (PSDs) due to certain microphysical processes are exceedingly rare, polarimetric radars can be used to determine changes in the characteristics of PSDs remotely. Such polarimetric radar observations at S and C band reveal PSDs in hook echoes atypical of those expected for typical Oklahoma rainfall. These observations are presented in the following section. Section 3 provides a discussion of possible explanations of the unusual PSDs. In section 4, data from a special rapid-scan case are presented, allowing for a unique look at the evolution of the precipitation characteristics of a hook echo throughout the occlusion of the low-level mesocyclone. Section 5 summarizes the major conclusions and offers a conceptual model of the proposed hypotheses.

## 2. OBSERVATIONS

## 2.1 Scattergrams

Fig. 1 is a series of  $Z_H$ - $Z_{DR}$  scattergrams from four supercell cases. The data reveal similarities between the hook echo precipitation characteristics in each case. Notably, each storm’s hook echo produces numerous data points for  $Z_H$  above about 40-45 dBZ that have  $Z_{DR}$  values below what is expected in Oklahoma rainfall, as indicated by the Cao et al. (2008) relation. In Fig. 1a, the separation between these hook echo points and those from the rest of the storm are particularly striking. Such  $Z_H$ - $Z_{DR}$  pairs indicate a trend towards particle size distributions with more spherical scatterers than is typical in Oklahoma rainfall. Analysis of the  $\rho_{HV}$  values of these points strongly suggests that the radar resolution volumes were sampling rainfall (not shown). Thus, some of the measurements in hook echoes reveal DSDs with larger-than-expected concentrations of smaller drops (and/or a lack of larger drops). Each case also produces hook echo points with large ( $> 3$  dB)  $Z_{DR}$  for  $Z_H$  as low as 20 dBZ up to 60 dBZ. The “large drop” points for lower  $Z_H$  values indicate a DSD skewed towards a sparse concentration of large drops and a relative deficit of small drops, a characteristic sign of size sorting.

Also of note in Figs. 1b,c is the protrusion of points towards the lower right of the panel (i.e., large  $Z_H$  and negative  $Z_{DR}$ ), likely indicative of large and giant hail (e.g., see Kumjian et al. 2010a, this conference). The appearance of such  $Z_H$ - $Z_{DR}$  pairs for large hail is periodic in some of the cases. Of the cases shown, such points are not present for two cases in which a long-track significant ( $> F-2$ ) tornado was occurring (Figs. 1a,d). In the nontornadic case (Fig. 1c), the points were more consistent throughout the lifetime of the storm, in agreement with Kumjian and Ryzhkov (2008) who claim that the hail signature is more consistent in nontornadic supercells than tornadic supercells. The 31 March 2008 supercell just produced a weak tornado at the time of the scan (Fig. 1b). Between the “pre-tornado” and “post-tornado” scans, more of the high- $Z_H$ , low- $Z_{DR}$  points appeared. Thus, investigating the time series of precipitation characteristics in hook echoes may demonstrate a link to storm behavior and evolution.

---

\*Corresponding author: Matthew R. Kumjian, 120 David L. Boren Blvd., NWC Suite 4900, Norman, OK 73072. E-mail: matthew.kumjian@noaa.gov

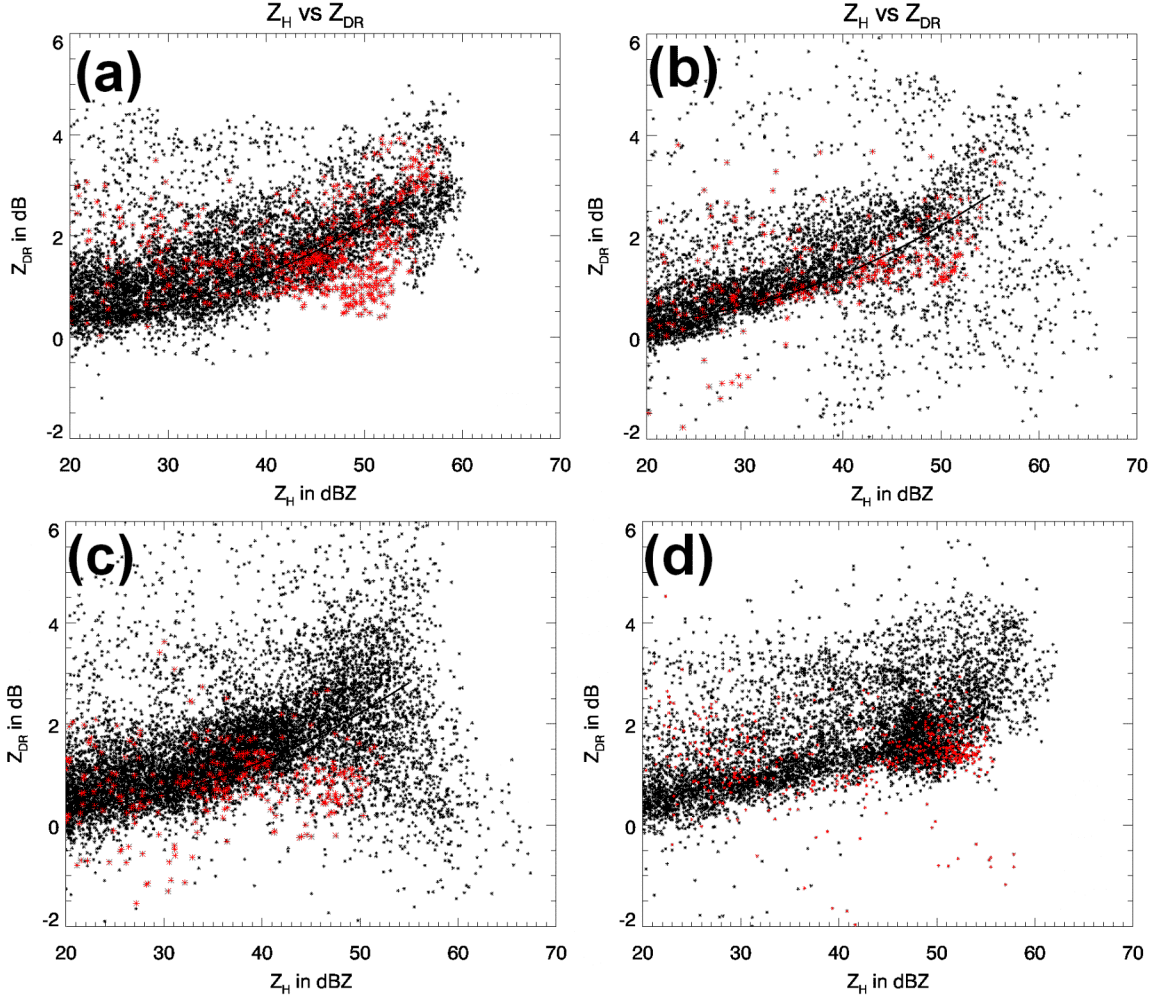


Fig. 1: Scattergrams of  $Z_H$  and  $Z_{DR}$  from four supercell cases: (a) 29 May 2004 at 0044 UTC; (b) 31 March 2008 at 0325 UTC; (c) 1 June 2008 at 0340 UTC; (d) 10 May 2003 at 0345 UTC. The black points represent data from the entire low-level scan of the storm, whereas the red points are those from the hook echo appendage. Data have been thresholded with  $\rho_{hv}$  to prevent contamination from the tornadic debris signature.

## 2.2 PPI Scans

The data reveal unusual DSDs in hook echoes, but also suggest large variability. Conventional presentation of the data in PPIs thus will provide insight into the spatial distribution and heterogeneities of precipitation characteristics in hook echoes, albeit in a less quantitative manner. What follows in this subsection is an investigation of low-level polarimetric radar scans of supercell hook echoes in selected cases where sufficiently high spatial resolution is achieved.

Low-level scans during a damaging long-track F3 tornado that struck Moore, OK on 10 May 2003 (Fig. 2) reveal complex patterns in the polarimetric variables. At the location of the tornado ( $x = 7$  km,  $y = 39$  km), a tornadic debris signature is evident as high  $Z_H$ , low  $Z_{DR}$ , and very low  $\rho_{hv}$  (Ryzhkov et al. 2005). A disrupted  $Z_{DR}$  arc (Kumjian and Ryzhkov 2008, 2009) is present along the southern edge of the forward-flank echo. High  $Z_{DR}$  values are seen wrapping around the western

side of the tornado, along the inner (inflow) edge of the  $Z_H$  hook echo. Behind the high- $Z_{DR}$  values, at the back of the hook echo and wrapping around the southern and southeastern sides of the tornado are regions of 45-55 dBZ with  $Z_{DR}$  less than 1.5 dB (and < 1 dB in some places). This region is also marked by high  $K_{DP}$ , indicating large liquid water content, and very high  $\rho_{hv}$ , indicating low diversity among hydrometeors and likely signifying rain. Thus, the polarimetric variables indicate distinct regions of large drops (in the  $Z_{DR}$  arc and extending around the inside edge of the hook echo) and smaller drops (back of hook echo and south and southeast of the tornado).

A similar pattern is observed in other cases, including another damaging (EF-4) tornado in Moore, OK on 10 May, this time in 2010 (Fig. 3). Data on this day were collected by both the S-band KOUN and the C-band University of Oklahoma Polarimetric Radar for Innovations in Meteorology and Engineering (OU-

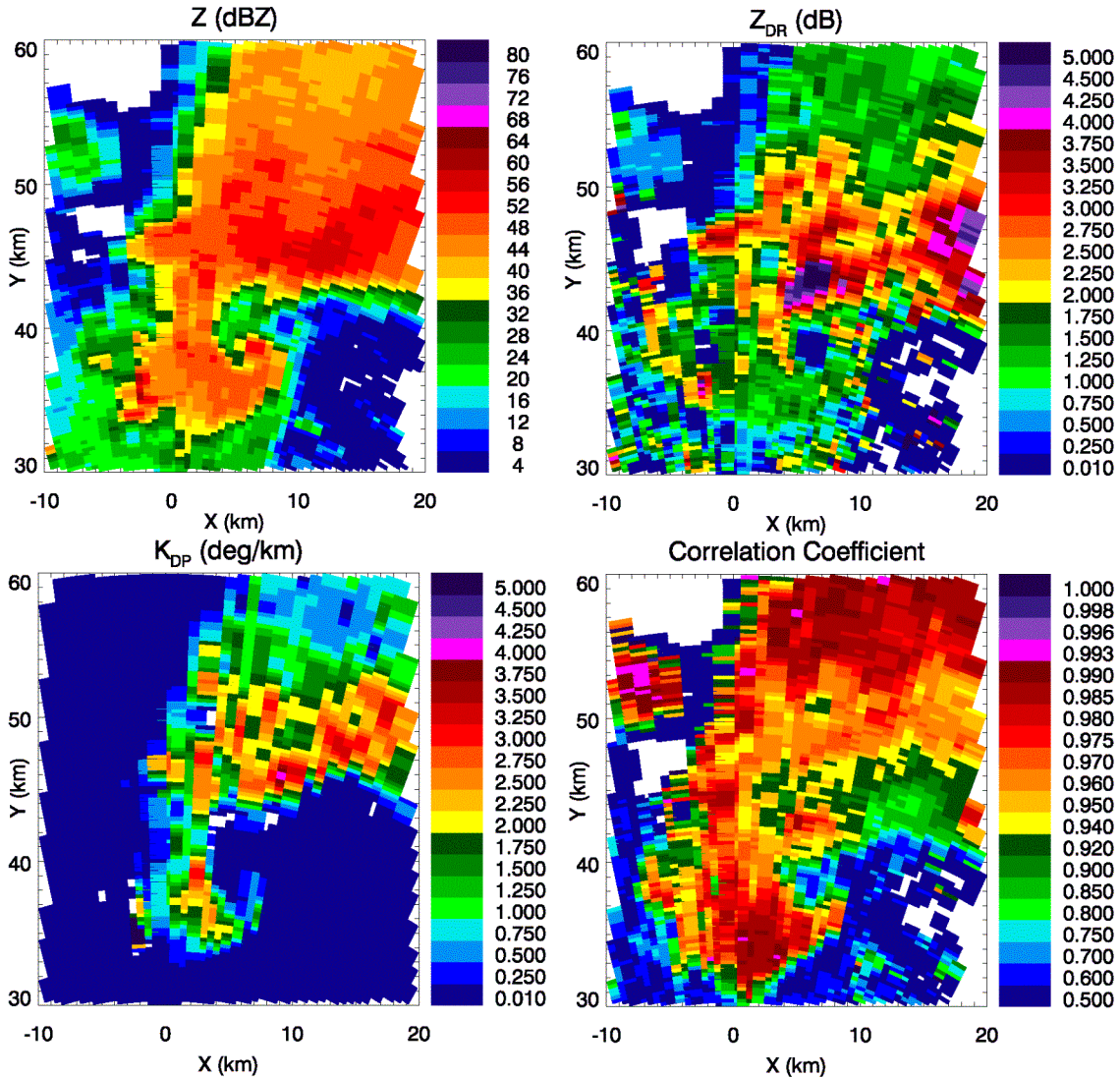


Fig. 2: Low-level PPI scan from 10 May 2003 at 0345 UTC, during a long-track damaging tornado (located at  $x = 7$  km,  $y = 39$  km). Fields of variables shown are (clockwise from top left)  $Z_H$ ,  $Z_{DR}$ ,  $K_{DP}$ , and  $\rho_{hv}$ .

PRIME; see Palmer et al. 2011). At C band, positive  $Z_{DR}$  signatures are enhanced due to resonant scattering by large raindrops; therefore, gradients in drop sizes will have more pronounced gradients in  $Z_{DR}$  at C band than at S band. Similarly,  $\rho_{hv}$  can be lower at C band, even in rain, due to Mie scattering effects (if large drops are present). In Fig. 3a, the tornado is at the center of the image, surrounded by bands of enhanced  $Z_H$ . In Fig. 3b, higher  $Z_{DR}$  is observed wrapping about three quarters of the way around the tornado, which is evident by the pronounced tornadic debris signature. On the southeastern quadrant of the circulation, however, a clear pocket of lower  $Z_{DR}$  (0 – 2 dB) is seen wrapping cyclonically into the tornado. This small-drop region is characterized by  $Z_H$  values between 35 – 45 dBZ, modest  $\Phi_{DP}$  ( $< 10^\circ$ ), and very high ( $> 0.975$ )  $\rho_{hv}$ .

About eleven minutes later, another destructive tornado (eventual EF-4) developed just 200 yards south of the National Weather Center, in Norman. The extremely close proximity to OU-PRIME affords a unique view of the storm, especially the hook echo and tornado (Fig. 4) that were captured with very high spatial resolution (Palmer et al. 2011; also Bodine et al. 2010, this conference). The hook echo from this particular storm is extremely thin, less than 1 km wide at its narrowest point (Fig. 4a). At the end of the hook echo, a debris ball of high  $Z_H$ , low  $Z_{DR}$ , and very low  $\rho_{hv}$  is observed. Even the “eye” of the tornado is apparent, likely due to a combination of centrifuging of debris (e.g., Dowell et al. 2005) and subsidence in the core of the vortex. Along the hook echo, a striking gradient in  $Z_{DR}$  and  $\rho_{hv}$  is evident (Fig. 4b,c), with very large drops located along the inner edge of the hook,

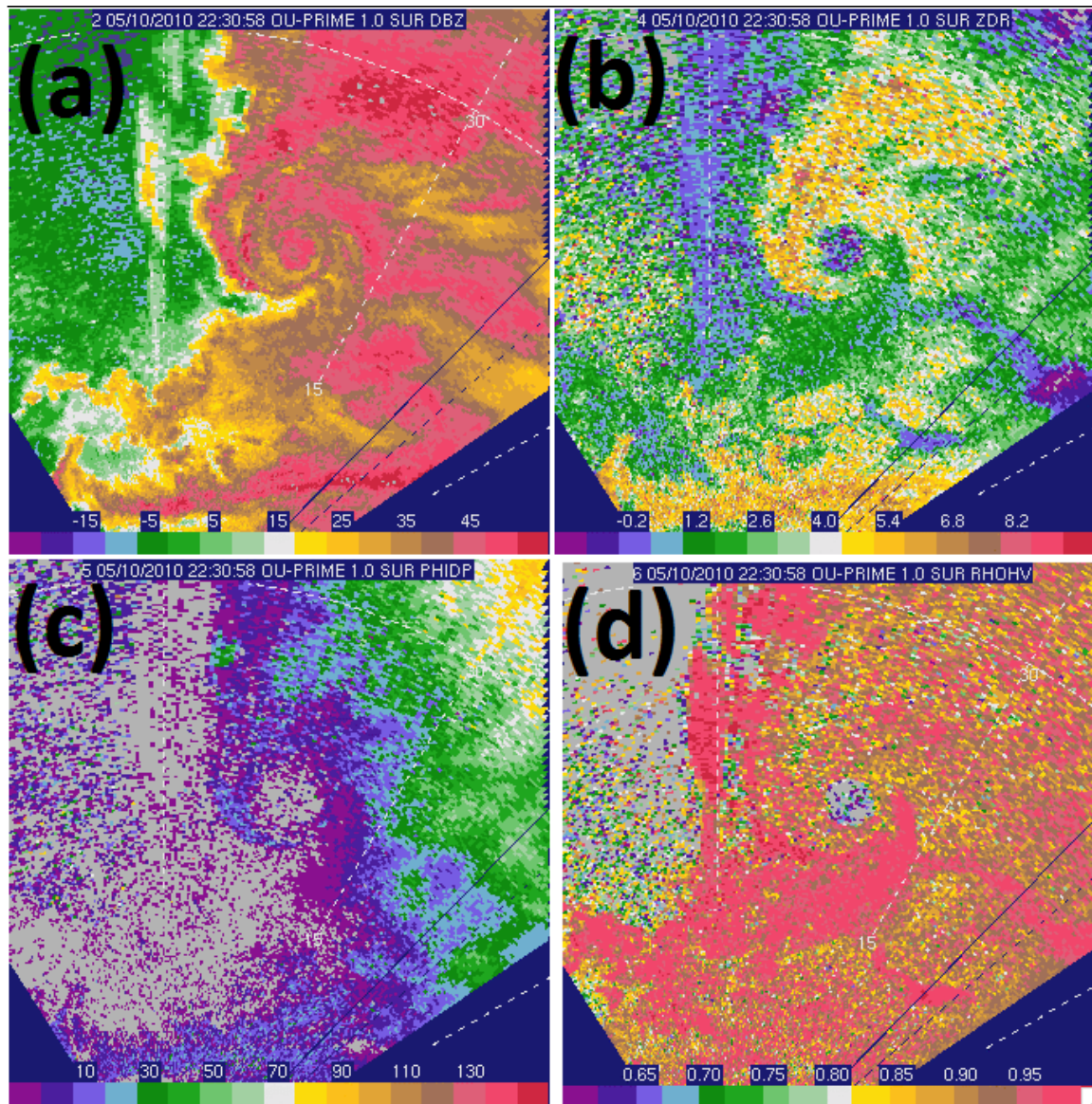


Fig. 3: Observed fields of (a)  $Z_H$ , (b)  $Z_{DR}$ , (c)  $\Phi_{DP}$ , and (d)  $\rho_{hv}$ , from 10 May 2010, at 2231 UTC. Data from the C-band OU-PRIME at 1.0° elevation (beamheight at the location of the tornado is about 400 m AGL).

with considerably smaller drops along the back edge (and extending farther north to the rear of the storm). Though  $Z_{DR}$  is low to the south and southeast of the tornado, as in the other cases, the  $\rho_{hv}$  is also considerably lower than expected in pure rain. It is likely that light debris was being lofted by the strong RFD winds, as blowing dust was visible from the National Weather Center.

At the same time, the Norman supercell storm produced at least two other tornadoes. The first was a brief EF-1 tornado that was possibly anticyclonic. The second was another cyclonic tornado (EF-2) that formed farther out along the rear-flank gust front in the absence of any appreciable precipitation echoes aloft. It is speculated that intense convergence along the rear-

flank gust front (evident in Doppler velocities, not shown) contributed to the “stretching” of pre-existing vertical vorticity to tornado strength. Precipitation-sized particles formed in the intense updraft associated with the aforementioned convergence and reached the surface only after the tornado was fully developed. The first drops to reach the surface would be the largest, via differential sedimentation, resulting in the low  $Z_H$  and high  $Z_{DR}$  observed near the tornado (Fig. 4b). Whereas the other cases have a region of small drops to the south and east of the tornado, in this case there were no precipitation-sized particles present at these locations. This lack of small raindrops may be owing to a lack of sufficient small-drop production at low levels (i.e., drops were located farther aloft still).

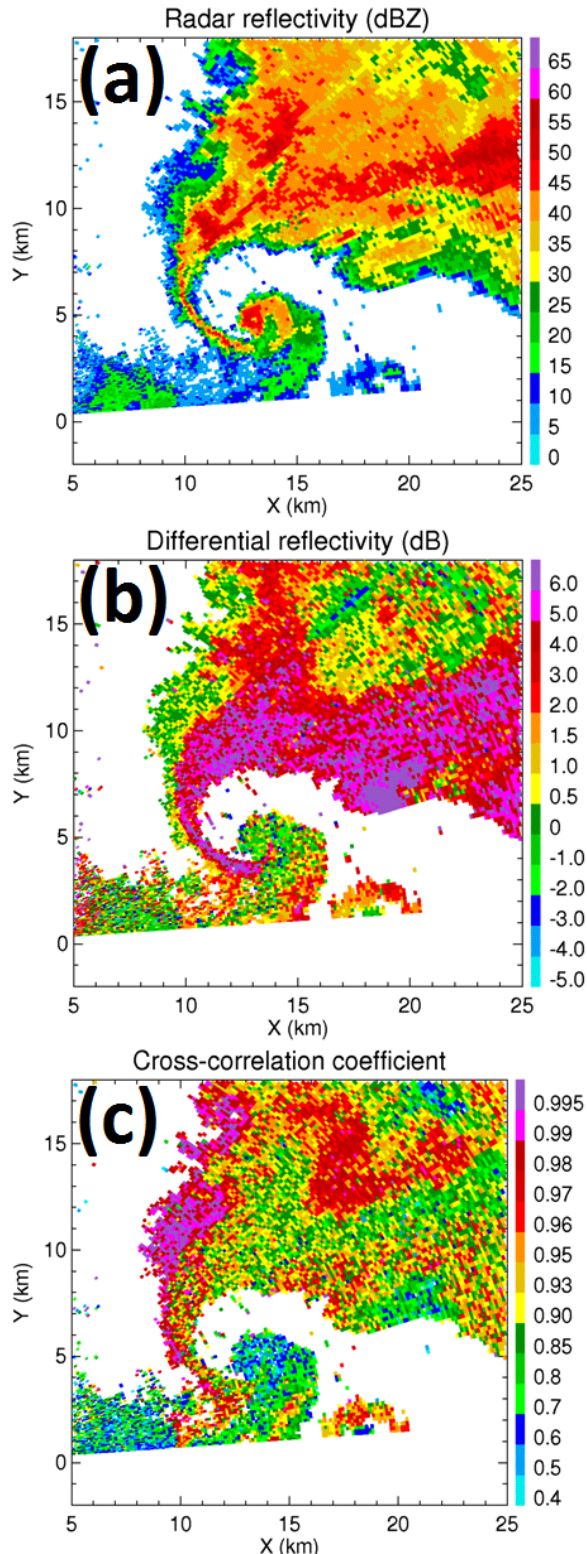


Fig. 4: Observed fields of (a)  $Z_H$ , (b)  $Z_{DR}$ , and (c)  $\rho_{hw}$  from 10 May 2010, at 2242 UTC. Data from the C-band OU-PRIME. The main tornado is located at about  $x = 13$  km,  $y = 5$  km. Another tornado is partly cut off by the sector, located at about  $x = 18.5$ ,  $y = 1.5$  km.

### 3. DISCUSSION AND EXPLANATION

Though a given  $Z_H$ - $Z_{DR}$  data point in a hook echo is possible in other precipitation systems, the collective dataset demonstrates the atypical nature of hook echo DSDs (Fig. 5). The consistent localization of regions of small and large drops in hook echoes inferred from the polarimetric radar data PPIs suggests similar mechanisms at work in each case, such as a microphysical or dynamic process intrinsic to supercells. But are these processes unique to supercells? One approach to this question is to look at the DSDs themselves; in other words, how similar or dissimilar are DSDs in supercell hook echoes to DSDs in other precipitating systems?

Anecdotally, numerous scientists and storm chasers have made eyewitness reports of very small drops in hook echoes and very large drops at the edge of the forward flank, consistent with the polarimetric radar observations presented here. At the time of this writing, the only published study to observe the DSD in a supercell RFD using a disdrometer is Schuur et al. (2001), who state that the resulting DSD “had a much larger small drop [ $< 1$  mm in diameter] concentration than was measured for any of the previous three cases” they investigated. More measurements of this kind are needed. Encouragingly, preliminary results from VORTEX-2 disdrometer measurements will be presented at this conference (Dawson and Romine 2010). Though such observations are limited, they provide some evidence that DSDs in hook echoes are unique, suggesting that processes distinctive to supercell storms may be involved. Hypotheses describing plausible explanations rooted in supercell microphysics and dynamics are presented in the next subsections. The relative merits of each are discussed.

#### 3.1 Hypotheses explaining small-drop-dominant DSDs

##### A) SATURATED CONDITIONS – NO EVAPORATION

Typically, large numbers of very small ( $< 1$  mm) drops are not observed at the surface. One major reason for this is that these tiny drops often evaporate before reaching the ground, owing to very small fall speeds ( $< 1$  m  $s^{-1}$ ) and preferential evaporation of smaller sizes (change in size  $D$  owing to evaporation  $dD/dt \sim D^{-1}$ ). The slow descent of tiny drops provides ample time for evaporation to take place. If supercell RFDs were saturated, no evaporation would take place and the small drops would be able to fall to the surface without being depleted by evaporation.

This hypothesis seems very unlikely, as RFDs are rarely (if ever) saturated. In fact, the surface thermodynamic observations by Markowski et al.

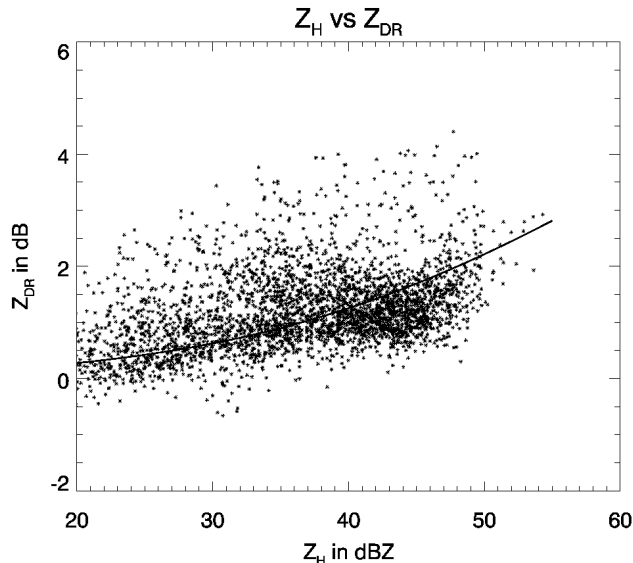


Fig. 5:  $Z_H$ - $Z_{DR}$  points from the hook echo of the 1 June 2008 supercell, observed at low levels (below 1 km AGL). Data are from a twenty-minute period 0332 – 0352 UTC and are thresholded with a minimum  $\rho_{hv}$  of 0.95. Overlaid is the Cao et al. (2008) curve for typical rainfall in Oklahoma.

(2002) essentially rule out this possibility. Also, other cases of heavy precipitation (in which evaporation is insignificant) should also display anomalously large concentrations of small drops, yet such cases have not been documented.

#### B) ENHANCED BREAK-UP

Another possible explanation for the abundance of small drops is that the wind fields in and around supercell mesocyclones are such that collisional drop break-up is enhanced. Strong gradients of updraft and downdraft, strong rotation, and turbulence in supercells could alter substantially the fall speeds of particles, which would affect the rates of collision and subsequent drop breakup (for example, see Low and List 1982; Brown 1986; Seifert et al. 2005).

Such enhanced breakup of large drops would result in significant raindrop multiplication, especially for smaller sizes. In some mesoscale convective systems, the surging outflow gust front carries with it tiny drops, ahead of the precipitation line. It is possible that such fragments are produced by similar mechanisms described above in the strong outflow winds. However, radar and disdrometer observations (Schuur et al. 2001) show that supercell hook echoes *still* contain very large drops, which suggests that breakup of these large drops is not a dominant process.

#### C) DYNAMICALLY-INDUCED DOWNDRAFTS

If the DSDs in supercell hook echoes are in fact unique to supercells, one should look at microphysical and kinematic features that are unique to such storms.

A major difference between supercells and other storm types is the large influence of pressure perturbations on the storm's evolution. In particular, vertically-directed perturbation pressure gradient forces (VPPGFs) are known to play a role in the production or maintenance of the RFD (e.g., Lemon and Doswell 1979; Markowski 2002). VPPGFs can arise from the interaction of strong environmental shear and the storm's updraft. Also, vertical gradients in vertical vorticity are associated with VPPGFs. A striking example of the latter is the "occlusion downdraft" (Klemp and Rotunno 1983), which forms when low-level vertical vorticity has amplified such that it exceeds the vertical vorticity aloft, resulting in a downward-directed VPPGF. The occlusion downdraft is a localized enhancement of the RFD, sometimes visually manifested as a "clear slot" that forms to the south or southeast of the center of circulation (e.g., Markowski 2002).

These dynamically-driven downdrafts are distinctive in supercell storms. In most other precipitation systems, downdrafts develop owing to negative buoyancy production via a combination of evaporation of raindrops, melting of hailstones, and precipitation loading. Evaporation acts preferentially on smaller raindrops; thus, the smallest raindrops rarely make it to the surface, as described above. However, if a downdraft is at least partly attributable to dynamic effects, the smaller drops may be transported downwards faster than they would normally fall. Indications that RFD air is comprised of parcels recycled from the boundary layer (Markowski et al. 2002) rather than mixing from dry air aloft suggest that the RFD remains relatively moist. Thus, in supercell RFDs the low lifting condensation levels (LCLs) and strong downdrafts can combine to rapidly transport smaller drops to lower levels than those at which they would otherwise be present.

Interestingly, the location of the small-drop regions of hook echoes corresponds to the expected locations of downdrafts (Fig. 6) in supercells. That is, on the rear side of the hook echo, wrapping around the southern and southeastern sides of the circulation (cf. Figs. 2-4). Also of note is that the high- $Z_{DR}$  regions correspond to the locations of expected updraft. In other words, size sorting is responsible for the large drop region: the large drops fall out at the periphery of the updraft, on the edge of the precipitation echo (hook echo in this case).

But if a dynamically-induced downdraft is transporting smaller drops to the surface (negative vertical advection), larger drops should also be transported to the surface. Radar measurements, especially those at C band, are very sensitive to the presence of large drops. The observations provided in the previous section do not indicate the presence of an appreciable concentration of large drops in these

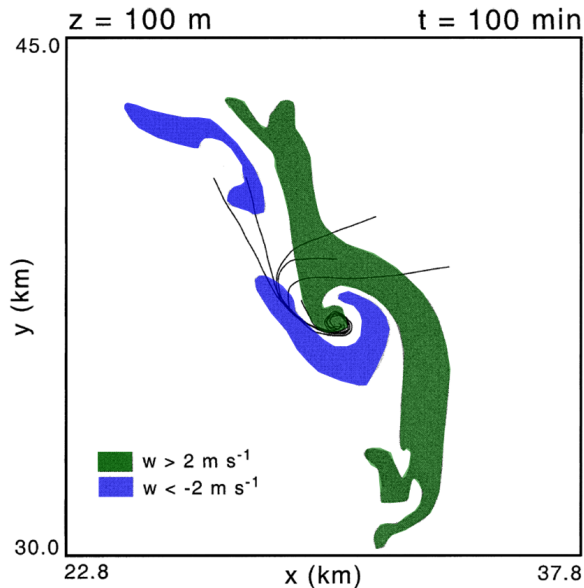


Fig. 6: Vertical velocity field and trajectories from a numerical simulation. Updraft regions are shown in green, downdrafts in blue. Adapted from Wicker and Wilhelmson (1995).

suspected downdrafts, as the observed  $Z_{DR}$  is quite low. This apparent discrepancy may be resolved by considering the air parcel trajectories included in Fig. 6. Wicker and Wilhelmson (1995) and others have found that a substantial portion of the air which ends up in a tornado comes from the forward-flank, as evidenced by the trajectories shown in Fig. 6. Recall that the  $Z_{DR}$  arc is characterized by a sparse population of large drops and a deficit of smaller drops. Kumjian and Ryzhkov (2008, 2009) interpret the signature as a result of vigorous size sorting owing to strong vertical wind shear. The tiny drops follow the airflow patterns very well owing to their small terminal fall speeds, whereas the larger drops simply fall out. Thus, if the trajectories in Fig. 6 are correct, small drops sorted from the  $Z_{DR}$  arc may be transported around the north side of the mesocyclone, where they enter the RFD and are transported to the ground. Precipitation trajectories based on dual-Doppler analyses or high-resolution numerical simulations may test this hypothesis.

### 3.2 Hypotheses explaining large-drop-dominant DSDs

#### A) EVAPORATION

Evaporation preferentially depletes the smaller drop sizes, which results in an increase in the median drop size and thus  $Z_{DR}$  (e.g., Li and Srivastava 2001; Kumjian and Ryzhkov 2010). Thus, an increase in  $Z_{DR}$  and decrease in  $Z_H$  is expected for DSDs that have undergone evaporation. However, Kumjian and Ryzhkov (2010) show that the magnitude of changes in

all polarimetric variables owing to evaporation alone are eclipsed by those induced by other processes, including size sorting. Additionally, small drops are located in close proximity to the large drop regions, which is not expected if evaporation is dominant. Therefore, evaporation is unlikely to be the main contributor to the observed regions of large drops.

#### B) SIZE SORTING

The regions of the hook echo typified by large  $Z_{DR}$  values (and thus large drops) have a more straightforward explanation. Size sorting can be invoked to explain the large  $Z_{DR}$  at the edge of the hook echo. Numerical simulations (Fig. 6) and dual-Doppler analyses indicate that the supercell updraft somewhat overlaps the inner edge of the hook (rainwater content in simulations, reflectivity factor in observations). Only the largest particles with the largest fall speeds can fall against the updraft on its periphery. Also, as the raindrops are advected horizontally around the mesocyclone following trajectories described above, the largest drops fall out first owing to their large fall speeds. Therefore, size sorting provides a simple yet powerful explanation for the appearance of large-drop-dominant DSDs at the inflow edge of the hook echo. This high- $Z_{DR}$  region often wraps around and connects with the  $Z_{DR}$  arc along the edge of the forward flank, which is also likely a result of size sorting (Kumjian and Ryzhkov 2008, 2009).

Size sorting owing to centrifuging by the mesocyclone can be ruled out. First, a simple scale analysis demonstrates that radial accelerations imparted on large drops by even strong mesocyclones are insufficient to displace the drops appreciable distances. Second, the small drops are located radially *farther* away from the center of circulation than the large drops. If centrifuging were occurring, the opposite would be true.

### 4. EVOLUTION OF DSDs

Generally, the four- to five-minute update times of WSR-88D radars are inadequate to capture the rapid evolution of storms. To mitigate this problem, Kumjian et al. (2010b) recently obtained polarimetric data using a rapid-scan strategy on a cyclic nontornadic supercell that moved through west-central Oklahoma on 1 June 2008. Full volume updates were achieved every 72 seconds, and oversampling in azimuth allowed for increased spatial resolution as well. This unique dataset provides the opportunity to examine the evolution of the hook echo DSDs at finer temporal scales than previously available.

For the sake of comparison, a quasi-quantitative measure is introduced. For each  $Z_H$  value, the Cao et

al. (2008) relation provides the “expected”  $Z_{DR}$  value typical of rainfall in Oklahoma:

$$Z_{DR} = 10^{(-2.6857 \cdot 10^{-4} Z_H^2 + 0.04892 Z_H - 1.4287)} \quad (1)$$

The “expected”  $Z_{DR}$  computed from eqn. (1) is compared to the observed  $Z_{DR}$  in the 1 June storm. Data from the 1 June supercell hook echo were subjected to a  $\rho_{hv}$  threshold of 0.95 to ensure the data points are mainly from rain. The correlation coefficient  $r$  between the expected and observed  $Z_{DR}$  values is then computed, providing a measure of similitude of hook echo rainfall to typical Oklahoma rainfall. Note that no strong correlations are expected because the atypical nature of hook echo DSDs has already been demonstrated. Rather, any patterns or trends in the correlation are of interest, especially if these are related to storm evolution.

Fig. 7 is a time series of the correlation coefficient  $r$  over a twenty-minute period beginning at 0331:52 UTC. It is clear that  $r$  is weakly positive for most of the analyzed times. There is a slight increase in  $r$  from the beginning of the period until 0343:55 UTC, when  $r$  reaches its maximum value ( $r = 0.647$ ). The maximum is followed by a precipitous decline that reaches a minimum value ( $r = -0.095$ ) at 0348:45 UTC, after which values return to their typical range.

The 0331:52 – 0352:52 UTC time period was selected because it encompasses an occlusion cycle, an important process in which rapid changes in storm structure occur. Notably, the maximum in  $r$  coincides with the occlusion of a low-level mesocyclone and RFD surge. The  $Z_H$  hook echo displays the characteristic “kinked” shape (Fig. 8) discussed in Beck et al. (2006). During the increase in  $r$ , close examination of the data (Fig. 9) reveals that the number of points above the one-to-one line decreases, indicating that the low- $Z_H$  (and thus low expected  $Z_{DR}$ ) and high observed  $Z_{DR}$  points decrease. Such high- $Z_{DR}$ , low- $Z_H$  points are typical of size sorting; a decrease in these points may be a result of a weakening updraft. As the mesocyclone shifts rearward and the hook echo kinks (0341:30 – 0345:08), the number of data points indicating smaller than expected drop sizes increase, especially in the region of Cao et al.  $Z_{DR} < 2$  dB and observed  $Z_{DR} < 1$  dB. An intensifying RFD that instigates the occlusion is capable of transporting more small drops by the mechanisms described above. At the apex of the kink,  $Z_H$  has decreased substantially, indicating that precipitation pathways into this region are disrupted.

Once the old mesocyclone is fully occluded,  $Z_H$  in the hook echo begins to increase again as it takes on its distinctive cyclonically-curved shape. At the same time,  $Z_{DR}$  increases substantially near the top of the hook echo, where it connects to the main body of

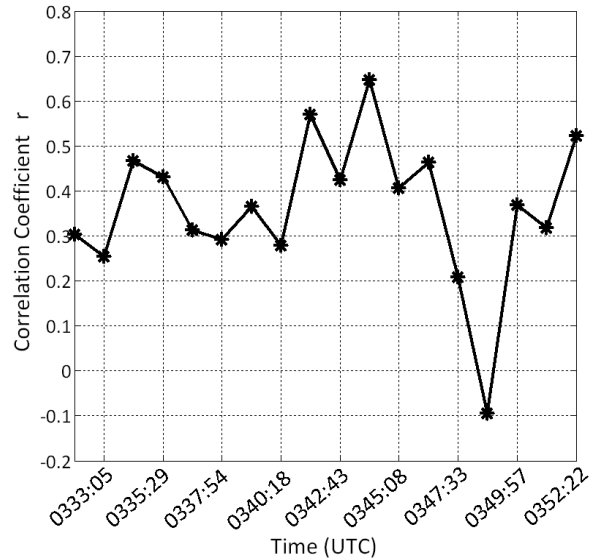


Fig. 7: Correlation coefficient  $r$  between the expected  $Z_{DR}$  calculated from (1) and the observed  $Z_{DR}$  in the hook echo of the 1 June 2008 storm. Data from the period 0331:52 – 0352:22 UTC are shown.

the storm. This increase in  $Z_{DR}$  associated with low-moderate  $Z_H$  causes the strong drop in correlation  $r$ . A re-intensification of the updraft as the new mesocyclone becomes established may be enhancing the  $Z_{DR}$  through sorting of the new drops falling into the hook as that pathway is re-opened.

Though the trends are weak and shown for only one case, there is at least some suggestion that the hook echo precipitation characteristics are linked to the storm’s behavior, especially the occlusion process. Increases in updraft strength (inferred from the  $Z_{DR}$  column) have been associated with a 10 – 20 minute lagged intensification of the precipitation core at low-levels in Picca and Ryzhkov (2010) and Picca et al. (2010, this conference). Thus, it seems plausible that changes in the hook echo precipitation characteristics inferred from polarimetric measurements may be related to storm behavior, including occlusion of the mesocyclone, RFD surges, and changes in low-level updraft strength, albeit at smaller lags. This interesting possibility warrants future investigations with data of sufficient spatial and temporal resolution to capture the rapid, fine-scale changes in hook echoes.

## 5. SUMMARY OF CONCLUSIONS

This study investigated the characteristics of hook echo precipitation through the use of S- and C-band dual-polarization radar observations of tornadic and nontornadic supercells. Special cases of storms in close proximity to the radar or scanned with rapid sampling

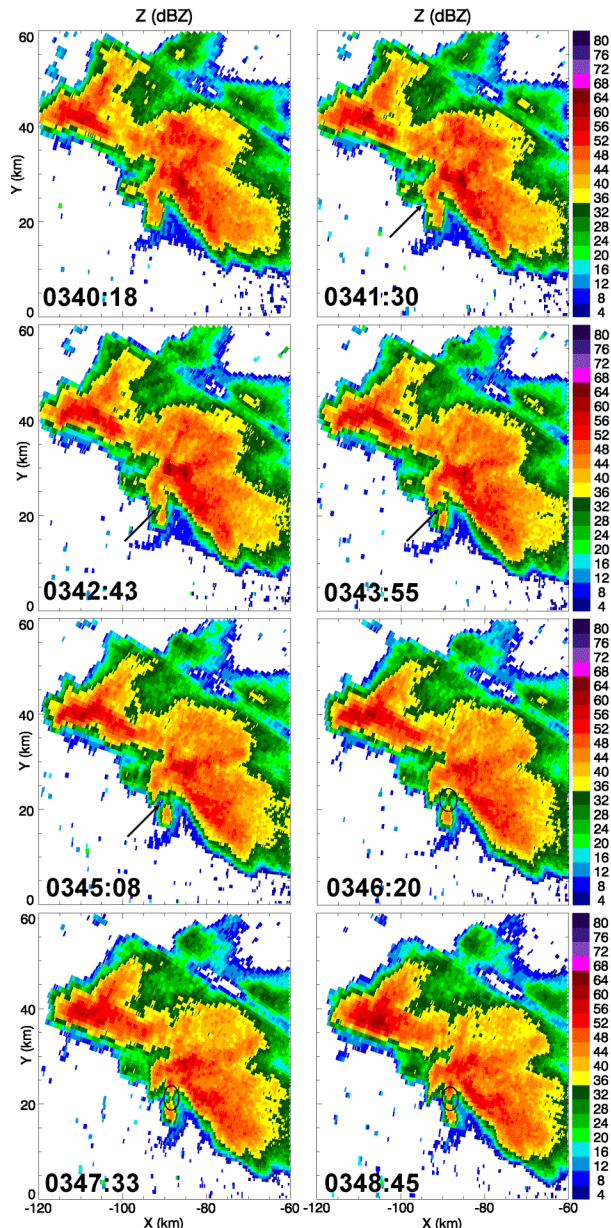


Fig. 8: Low-level  $Z_H$  from 1 June 2008, at 0340:18 – 0348:45 UTC. Arrows indicate the “kink” in the hook echo, and circles represent areas of regeneration of  $Z_H$  (and very high  $Z_{DR}$ ).

techniques afforded enhanced spatial and temporal resolution. The following key points were reached:

- 1) Drop size distributions (DSDs) in supercell hook echoes are exotic and atypical of rainfall in Oklahoma from other precipitating systems.
- 2) DSDs in hook echoes are spatially inhomogeneous, with large drop regions located on the inner/inflow edge and regions of very small drops located at the

back of the hook that wrap around the southern and southeastern sides of the circulation.

- 3) The large drop regions are likely a result of size sorting owing to the low-level updraft as only the largest drops are able to fall out of the updraft periphery.
- 4) The small drop regions may be owing to dynamically-induced downdrafts that transport the drops to the surface more rapidly than they would otherwise fall, preventing total depletion of the small drops by evaporation.
- 5) There is some evidence suggesting that the anomalously large concentrations of small drops in supercell hook echoes are unique to such storms.
- 6) There exist weak trends in the DSD characteristics that may be related to the occlusion process, including the rearward movement of the mesocyclone, RFD surge, and updraft weakening.

A schematic conceptual model of the hook echo polarimetric features and vertical velocity fields is provided in Fig. 10. Future studies, especially those employing high-resolution dual-polarization radars or taking *in situ* measurements with disdrometers, may provide more definitive evidence for the conclusions above. The gradient of drop sizes across the hook echo is a feature that bulk single-moment microphysics parameterizations are unable to reproduce, which may have implications for the thermodynamic characteristics of simulated RFDs, which are important for tornadogenesis. A better understanding of the links between supercell dynamics and the unique DSDs in hook echoes is warranted, especially if the microphysics is tied to storm evolution and behavior, as suggested in this study.

## 6. ACKNOWLEDGMENTS

The NSSL/CIMMS staff who worked to ensure high-quality operation of KOUN is thanked. Funding for this study comes from NOAA/University of Oklahoma Cooperative Agreement NA17RJ1227 under the U.S. Dept. of Commerce. Some of the data presented were collected for research funded by NSF grant ATM-0532107. We thank David Bodine for providing one of the OU-PRIME figures. OU-PRIME is maintained and operated by the Atmospheric Radar Research Center (ARRC) of the University of Oklahoma. Thoughtful discussions with Alex Schenkman and Chad Shafer (OU) and Dan Dawson (NSSL) contributed to the study.

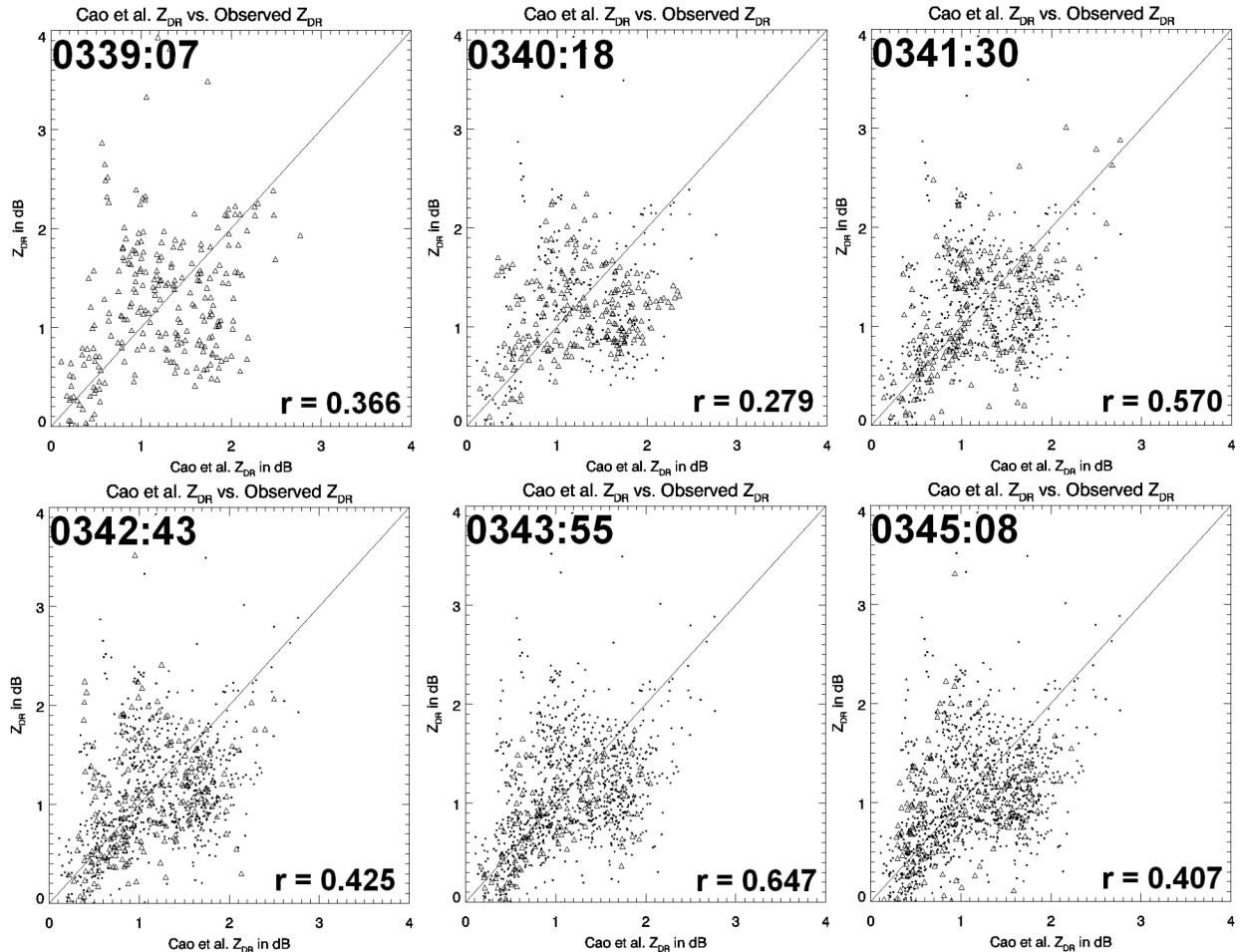


Fig. 9: Scattergrams of the “Cao et al.” (expected)  $Z_{DR}$  versus the observed  $Z_{DR}$  from the 1 June 2008 supercell hook echo. Each panel shows data from consecutive scans (times indicated in UTC in the upper left). Data points from the current time are plotted as triangles, and all previous times are shown as dots. The correlation coefficient  $r$  is indicated in the bottom right of each panel.

## 7. REFERENCES

- Beck, J.R., J.L. Schroeder, and J.M. Wurman, 2006: High-Resolution Dual-Doppler Analyses of the 29 May 2001 Kress, Texas, Cyclic Supercell. *Mon. Wea. Rev.*, **134**, 3125–3148.
- Bodine, D., R.D. Palmer, M.R. Kumjian, and A.V. Ryzhkov, 2010: High-resolution OU-PRIME radar observations of a prolific tornado-producing supercell on 10 May 2010. *25<sup>th</sup> Conf. on Severe Local Storms*, Denver, CO, Amer. Meteor. Soc., P8.4.
- Brown, P.S., 1986: Parameterization of drop-spectrum evolution due to coalescence and breakup. *J. Atmos. Sci.*, **44**, 242–249.
- Cao, Q., G. Zhang, E. Brandes, T.J. Schuur, A.V. Ryzhkov, and K. Ikeda, 2008: Analysis of video disdrometer and polarimetric radar data to characterize rain microphysics in Oklahoma. *J. Appl. Meteor. and Climatology*, **47**, 2238–2255.
- Dawson, D.T., and G.S. Romine, 2010: A preliminary survey of DSD measurements collected during VORTEX-2. *25<sup>th</sup> Conf. on Severe Local Storms*, Denver, CO, Amer. Meteor. Soc., 8A.4.
- Dowell, D.C., C.R. Alexander, J.M. Wurman, and L.J. Wicker, 2005: Centrifuging of hydrometeors and debris in tornadoes: radar-reflectivity patterns and wind-measurement errors. *Mon. Wea. Rev.*, **133**, 1501–1524.
- Grzych, M.L., B.D. Lee, and C.A. Finley, 2007: Thermodynamic analysis of supercell rear-flank downdrafts from project ANSWERS. *Mon. Wea. Rev.*, **135**, 240–246.

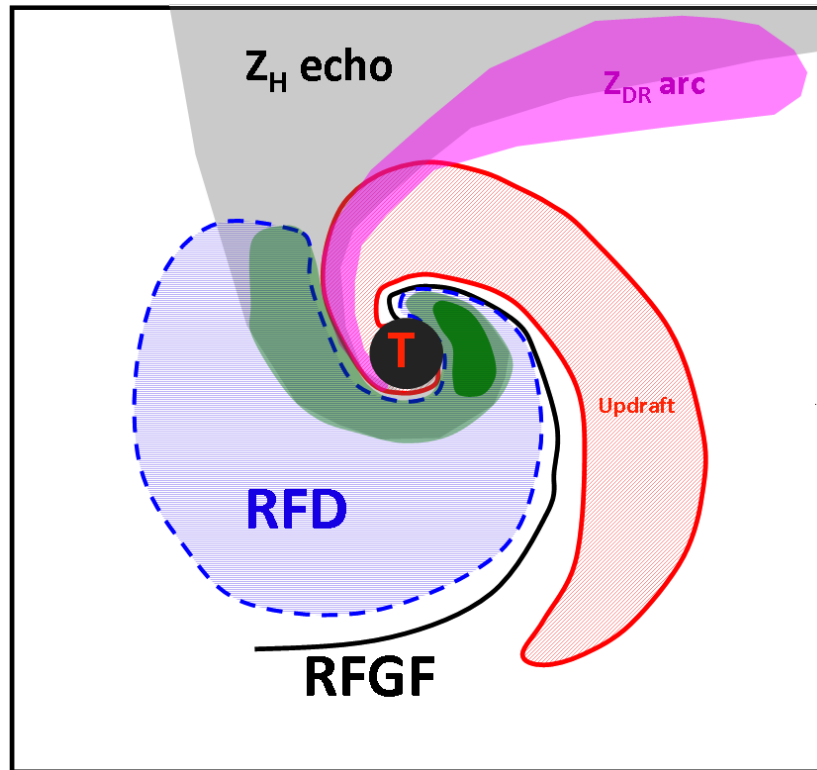


Fig. 10: Conceptual model of the precipitation characteristics of supercell hook echoes overlaid with the locations of updraft (red), RFD (blue), and the primary rear-flank gust front (black line, RFGF). The region shaded in pink indicates large-drop zones with high  $Z_{DR}$  (including the  $Z_{DR}$  arc). The green shading represents regions of lower  $Z_{DR}$  and smaller drop sizes. The dark green region represents an enhancement in tiny drops owing to the occlusion downdraft. The location of the tornado is indicated by the black circle with a red "T".

Klemp, J.B., and R. Rotunno, 1983: A study of the tornadic region within a supercell thunderstorm. *J. Atmos. Sci.*, **40**, 359-377.

Kumjian, M.R., and A.V. Ryzhkov, 2008: Polarimetric signatures in supercell thunderstorms. *J. Appl. Meteor. and Climatology*, **47**, 1940-1961.

Kumjian, M.R. and A.V. Ryzhkov, 2009: Storm-relative helicity revealed from polarimetric radar observations. *J. Atmos. Sci.*, **66**, 667-685.

Kumjian, M.R., and A.V. Ryzhkov, 2010: The impact of evaporation on polarimetric characteristics of rain: Theoretical model and practical implications. *J. Appl. Meteor. and Climatology*, **49**, 1247-1267.

Kumjian, M.R., J.C. Picca, S.M. Ganson, A.V. Ryzhkov, J. Krause, and A.P. Khain, 2010a: Polarimetric radar characteristics of large hail. *25<sup>th</sup> Conf. on Severe Local Storms*, Denver, CO, Amer. Meteor. Soc., 11.2.

Kumjian, M.R., A.V. Ryzhkov, V. Melnikov, and T.J. Schuur, 2010b: Rapid-scan super-resolution observations of a cyclic supercell using a dual-polarization WSR-88D. *Mon. Wea. Rev.*, **138**, 3762-3786.

Lemon, L.R., and C.A. Doswell: Severe thunderstorm evolution and mesocyclone structure as related to tornadogenesis. *Mon. Wea. Rev.*, **107**, 1184-1197.

Li, X., and R.C. Srivastava, 2001: An analytical solution for raindrop evaporation and its application to radar rainfall measurements. *J. Appl. Meteor.*, **40**, 1607-1616.

Low, T.B., and R. List, 1982: Collision, coalescence, and breakup of raindrops. Part II: Parameterization of fragment size distributions. *J. Atmos. Sci.*, **39**, 1607-1618.

Markowski, P.M., 2002: Hook echoes and rear-flank downdrafts: A review. *Mon. Wea. Rev.*, **130**, 852-876.

- Markowski, P. M., J.M. Staka, E.N. Rasmussen, 2002: Direct surface thermodynamic observations within the rear-flank downdrafts of nontornadic and tornadic supercells. *Mon. Wea. Rev.*, **130**, 1692-1721.
- Markowski, P.M., J.M. Straka, and E.N. Rasmussen, 2003: Tornadogenesis resulting from the transport of circulation by a downdraft: Idealized numerical simulations. *J. Atmos. Sci.*, **60**, 795-823.
- Palmer, R.D., D. Bodine, M.R. Kumjian, B. Cheong, G. Zhang, Q. Cao, H.B. Bluestein, A. Ryzhkov, T.-Y. Yu, and Y. Wang, 2011: The 10 May 2010 tornado outbreak in central Oklahoma: Potential for new science with high-resolution polarimetric radar. *Bull. Amer. Meteor. Soc.*, **in review**.
- Picca, J.C., and A.V. Ryzhkov, 2010: Polarimetric signatures of melting hail at S and C bands: Detection and short-term forecast. *26<sup>th</sup> Conf. on Interactive Information and Processing Systems (IIPS)*, Atlanta, GA, Amer. Meteor. Soc., 10B.4
- Picca, J.C., M.R. Kumjian, and A.V. Ryzhkov, 2010:  $Z_{DR}$  columns as a predictive tool for hail growth and storm evolution. *25<sup>th</sup> Conf. on Severe Local Storms*, Denver, CO, Amer. Meteor. Soc., 11.3.
- Ryzhkov, A.V., T.J. Schuur, D.W. Burgess, and D.S. Zrnic, 2005: Polarimetric tornado detection. *J. Appl. Meteor.*, **44**, 557-570.
- Schuur, T.J., A.V. Ryzhkov, D.S. Zrnic, and M. Schönhuber, 2001: Drop size distributions measured by a 2D video disdrometer: Comparison with dual-polarization radar data. *J. Appl. Meteor.*, **40**, 1019-1034.
- Seifert, A., A. Khain, U. Blahak, and K.D. Beheng, 2005: Possible effects of collisional breakup on mixed-phase deep convection simulated by a spectral (bin) cloud model. *J. Atmos. Sci.*, **62**, 1917-1931.
- Wicker, L.J., and R.B. Wilhelmson, 1995: Simulation and analysis of tornado development and decay within a three-dimensional supercell storm. *J. Atmos. Sci.*, **52**, 2675-2703.